SANDIA REPORT

SAND2005-3994
Unlimited Release
Printed June 2005

Mold-filling Experiments for Validation of Modeling Encapsulation. Part 1: "Wine Glass" Mold

Lisa A. Mondy, Anne M. Grillet, Ray O. Cote, Jaime N. Castañeda, and Stephen Altobelli

Prepared by
Sandia National Laboratories
Albuquerque, New Mexico 87185 and Livermore, California 94550

Sandia is a multiprogram laboratory operated by Sandia Corporation, a Lockheed Martin Company, for the United States Department of Energy's National Nuclear Security Administration under Contract DE-AC04-94AL85000.

Issued by Sandia National Laboratories, operated for the United States Department of Energy by Sandia Corporation.

Available to DOE and DOE contractors from
U.S. Department of Energy
Office of Scientific and Technical Information
P.O. Box 62
Oak Ridge, TN 37831

Telephone: (865)576-8401
Facsimile: (865)576-5728
E-Mail: reports@adonis.osti.gov
Online ordering: http://www.osti.gov/bridge

Available to the public from
U.S. Department of Commerce
National Technical Information Service
5285 Port Royal Rd
Springfield, VA 22161

Telephone: (800)553-6847
Facsimile: (703)605-6900
E-Mail: orders@ntis.fedworld.gov
Online order: http://www.ntis.gov/help/ordermethods.asp?loc=7-4-0#online

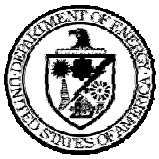

SAND2005-3994
Unlimited Release
Printed June 2005

Mold-filling experiments for validation of modeling encapsulation. Part 1: "Wine glass" mold.

Lisa A. Mondy
Multiphase Transport Processes

Anne M. Grillet, Ray O. Cote, Jaime N. Castañeda
Thermal/Fluid Experimental Sciences

Sandia National Laboratories
P.O. Box 5800
Albuquerque, NM 87185-0834

Stephen Altobelli
New Mexico Resonance
Suite C1
2301 Yale SE
Albuquerque, NM 87106-4237

Abstract

The C6 project "Encapsulation Processes" has been designed to obtain experimental measurements for discovery of phenomena critical to improving these processes, as well as data required in the verification and validation plan (Rao et al. 2001) for model validation of flow in progressively complex geometries. We have observed and recorded the flow of clear, Newtonian liquids and opaque, rheologically complex suspensions in two mold geometries. The first geometry is a simple wineglass geometry in a cylinder and is reported here in Part 1. The results in a more realistic encapsulation geometry are reported in Part 2.

Acknowledgments

The authors would like to acknowledge Rekha Rao and Tom Baer (9114) for invaluable help in designing validation studies. Thanks also go to Jeremy Barney (9112) for test-running the NMR mold filling apparatus.

Contents

Figures

Tables

This page intentionally left blank

1. Introduction

The C6 project "Encapsulation Processes" has been designed to obtain experimental measurements to provide better understanding of the free surface flow of suspensions into molds. The data obtained was also required by the ASCI Manufacturing Flows Physics Plan for model validation. We have observed and recorded the flow of clear, Newtonian liquids and opaque, rheologically complex suspensions in two mold geometries.

The first geometry tested was a simple cylindrical mold with a wine glass shape inside. Results of the earlier studies of a Newtonian liquid flowing around the wine glass shape were compared with numerical results in Baer et al. (2003). For completeness these studies are included in this report as well. The studies have been expanded to include non-Newtonian suspensions. We observed opaque suspensions that mimic some of the rheology of complex encapsulation materials such as "459" to record key features such as the shape of the free surface entering the mold (Adolf et al. 2000). This provided validation data for coupling free surface tracking algorithms (the level set method) with shear- and time-dependent fluid rheology. Other suspensions were also observed using nuclear magnetic resonance (NMR) imaging to determine particle concentration changes caused by the flow. This provides validation data for suspension constitutive equations such as the diffusive flux or suspension balance equations (Rao et al. 2002, Fang 2002), as well as the coupling of these rheological models with the level set method.

The second geometry is a mold with an outer shape more representative of the small square generator and several interior elements to represent internal parts. This second mold was made to closely match a more realistic mesh designed by Rekha Rao, Eric Lindgren, and Steve Montgomery (Wilkes and Rao, 2005). The flow of a transparent Newtonian oil and the opaque 459 simulant is recorded visually and reported in Part 2.

This page intentionally left blank.

2. Optical recordings of flow around a "Wine Glass"

2.1. Experimental details

The experimental geometry consists of a clear Plexiglas™ cylinder enclosing a "wine glass," also machined from Plexiglas™. Figure 1 is a sketch of the mold, showing the filling port towards the bottom of the mold. The diameter of the outer cylinder is about 4 cm and that of the filling port about 1 cm.

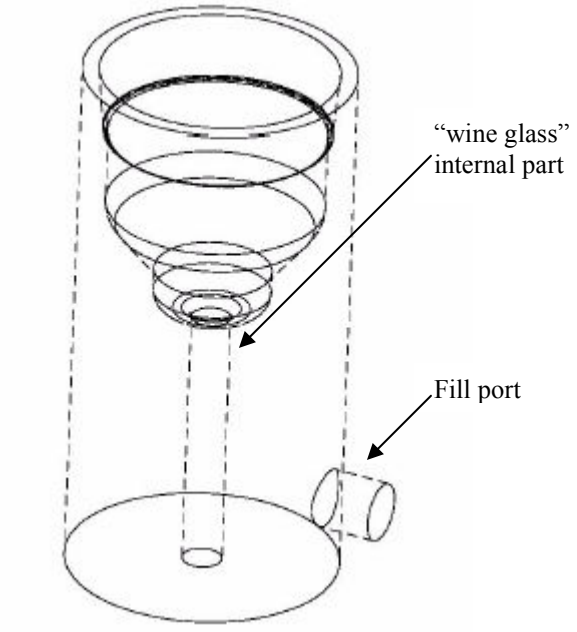

Figure 1. Sketch of simplified mold geometry

Three fluids were used, a lubricant UCON 75-H-90000 and two suspensions of tabular alumina (Alox) in Jeffamine T5000 or T403. These Jeffamine suspensions were used to simulate the rheological behavior of the encapsulant "459" without the added complexity of dealing with a polymerizing system (Adolf et al. 2000). The Alox used was a spare batch that did not meet the specifications for weapons use but could be used to create a model of the 459 encapsulant. The suspensions contained 45% by volume of the Alox particles. The higher viscosity suspension closely matched the viscosity of the UCON fluid. However, this suspension exhibited little of the non-Newtonian behavior typical of 459, so a less viscous version of the Jeffamine series was also used as a suspending liquid. Figures 2 and 3 show the viscosities of these three fluids.

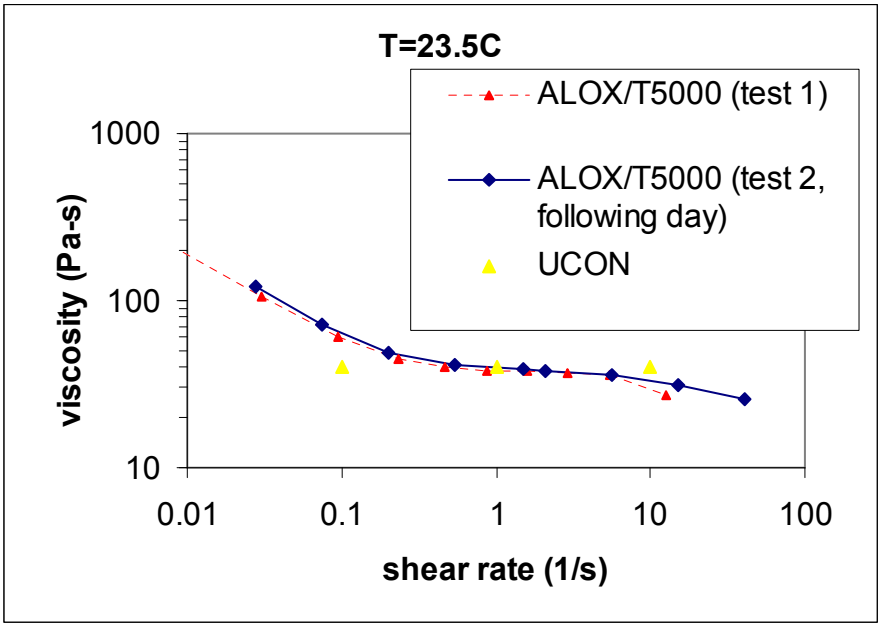

Figure 2. Viscosity of UCON lubricant 75-H-90000 compared to that of a suspension of T5000 and Alcoa tabular alumina (45% by volume)

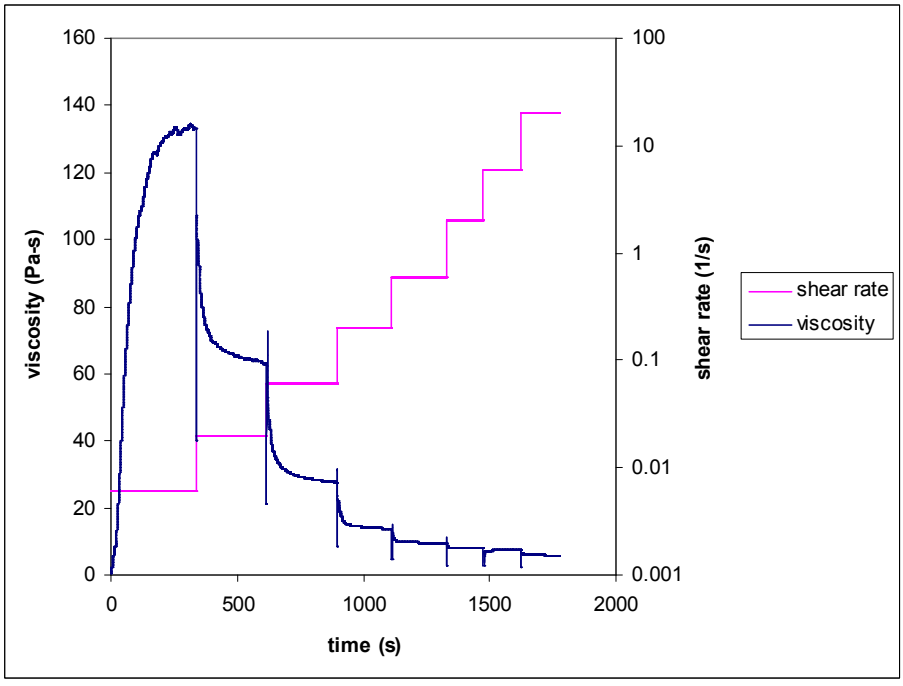

Figure 3. Viscosity of a suspension of T403 and Alcoa tabular alumina (45% by volume) showing time history effects and shear thinning typical of the encapsulant 459.

At 20°C, the density of the UCON fluid is 1.09 g/cm^3 and the densities of the Jeffamines T5000 and T403 are 1.00 and 0.98 g/cm^3, respectively . The intrinsic density of the Alox particles is 3.98 g/ cm^3.

We measured the surface tension and contact angle on glass and Plexiglas™ of these materials (Table 1). The contact angle was measured with a goniometer. The error in the contact angle measurement is estimated to be ±2-3°, except for the contact angle of the most viscous UCON 75-H-90000, which proved difficult to measure. The range of values obtained on Plexiglas™ is shown in the Table. An important caveat is that the technique is not very reliable for small contact angles (<20-25°). This makes measuring the Jeffamine based materials problematic. Therefore, to illustrate the differences between filled and unfilled materials we 1) tested an additional member of the Jeffamine, XTJ509, and 2) measured the contact angle on a low energy Teflon™ surface. The effect of adding suspended particles was inconsistent; in general when a low contact angle results, the particles increase the contact angle somewhat. However, as mentioned above these measurements are not reliable. The addition of suspended particles in Jeffamine T403 decreases the angle by about 10% on the Teflon™ surface. Because this high contact angle was more accurately measured, we feel that a slight increase in contact angle is more likely to be the general effect of adding particles.

The surface tension was measured with a Du Noüy ring (mean circumference of 5.935 cm). In a limited number of cases the contact angle was also measured using Goniometer images. These measurements are also listed in Table 1. In the cases in which more than one measurement was taken, the average is listed as well as the total range of the measurements.

Table 1. Wetting parameters

Material	**Contact Angle** Glass/Plexiglas™	**Surface Tension**
UCON 75-H-90000	27° / 31°-44°	42.4±0.1 dyne/cm
UCON 75-H-9500	43° /28°	43.1±1.2 dyne/cm
UCON 50-HB-5100	40° /26°	40.1±0.2 dyne/cm
Jeffamine T403	17° /16°	35.0 dyne/cm
Jeffamine XTJ509	-- / 8°	34.2 dyne/cm
AlOx suspension in T403	17° /18°	38.1 dyne/cm
AlOx suspension in XTJ509	-- /16°	38.4±0.7 dyne/cm
Material	**Contact Angle** Teflon™ Coating	
Jeffamine T403	101°	
AlOx suspension in T403	90°	

Fluid was introduced into the port from a reservoir, which was held at a constant nominal pressure of 2 psig with regulated house air. The entire apparatus rested upon a balance so

the actual flow rate could be determined. The liquid displaced air, which escaped through the open top of the mold.

The process was captured on video at a fixed frame rate of 30 fps. Therefore, the time since filling began could be calculated from the frame number. Three camera views were recorded simultaneously. One was chosen to show the shape of the free surface during the early time as the material entered through the filling port. Another was a view up the bottom of the transparent mold to show the material flowing around the wine glass stem. The final camera view showed the mass of the material to monitor the flow rate.

2.2. Results

Some suggested metrics to be used to validate numerical models include:

- Time versus filled weight
- Time for the lobes of fluid to meet around the base of the wine glass (a "knit line" beginning to form)
- Time for the bottom of mold to be filled (the complete disappearance of the void left near the wall opposite the fill tube – such a void can still be seen in Figure 5 at 45 s and in Figure 7 at 5.33 s)
- Shape of the interface over time

The resulting fill rates are shown in Figure 4.

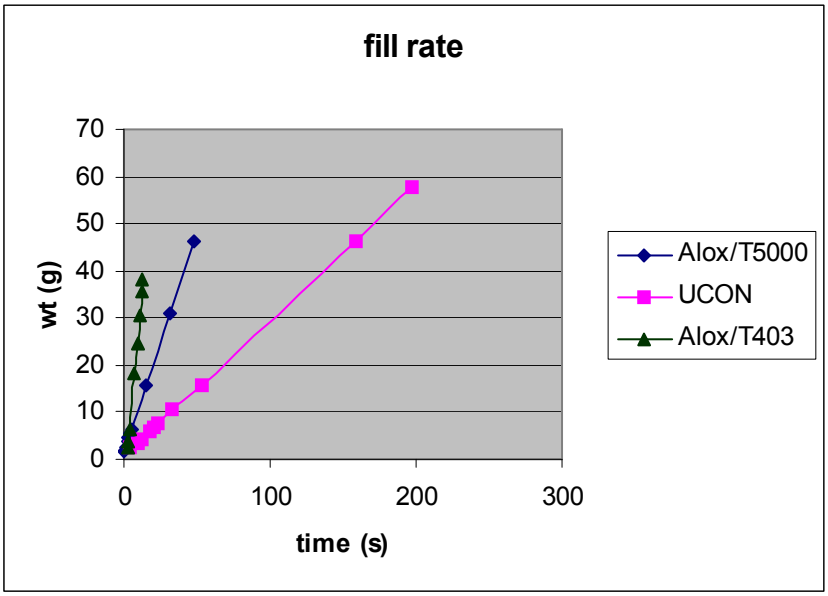

Figure 4. Mold fill rate for visual experiments.

Representative frames from the video of the process are shown in Figures 5 - 7. Figure 5 shows the shape of the most viscous Newtonian liquid used in the study, UCON 75H-90000. Time 0 is set to be the first frame in which liquid can be seen at the mouth of the fill port and the scale begins to record a rapid rise in weight. There is approximately a 10-

frame uncertainty (0.3 s) uncertainty in this initial time; therefore, the time metrics listed below also include this error.

From the video represented in Figure 5, the time at which the two lobes of liquid rejoin after flowing around the wine glass is at about 36.7 s. The advancing front hits the far edge of the bottom of the mold completely filling the view from the bottom at approximately 45.5 s.

Figure 6 shows the simplified mold being filled with the suspension of Alox in Jeffamine T5000. The error in the initial time is about the same (plus or minus 0.3 s) as in the previous experiment. Here, at approximately 21.3 s the fluid first comes together after traveling around the wine glass stem. The advancing front reaches completely fills the bottom of the mold at about 29.3 s.

Finally, Figure 7 gives representative frames from a video of the mold being filled with the suspension of Alox in Jeffamine T403. Because the viscosity is much lower, the mold filled much faster. However, in this case it is clear which frame is the first in which liquid emerges; therefore, there is only about a 0.03 s uncertainty in the initial time. Again, the times for the knit lines to begin to form and the bottom to fill are 4.33 s and 4.53 s, plus or minus 0.03 s, respectively.

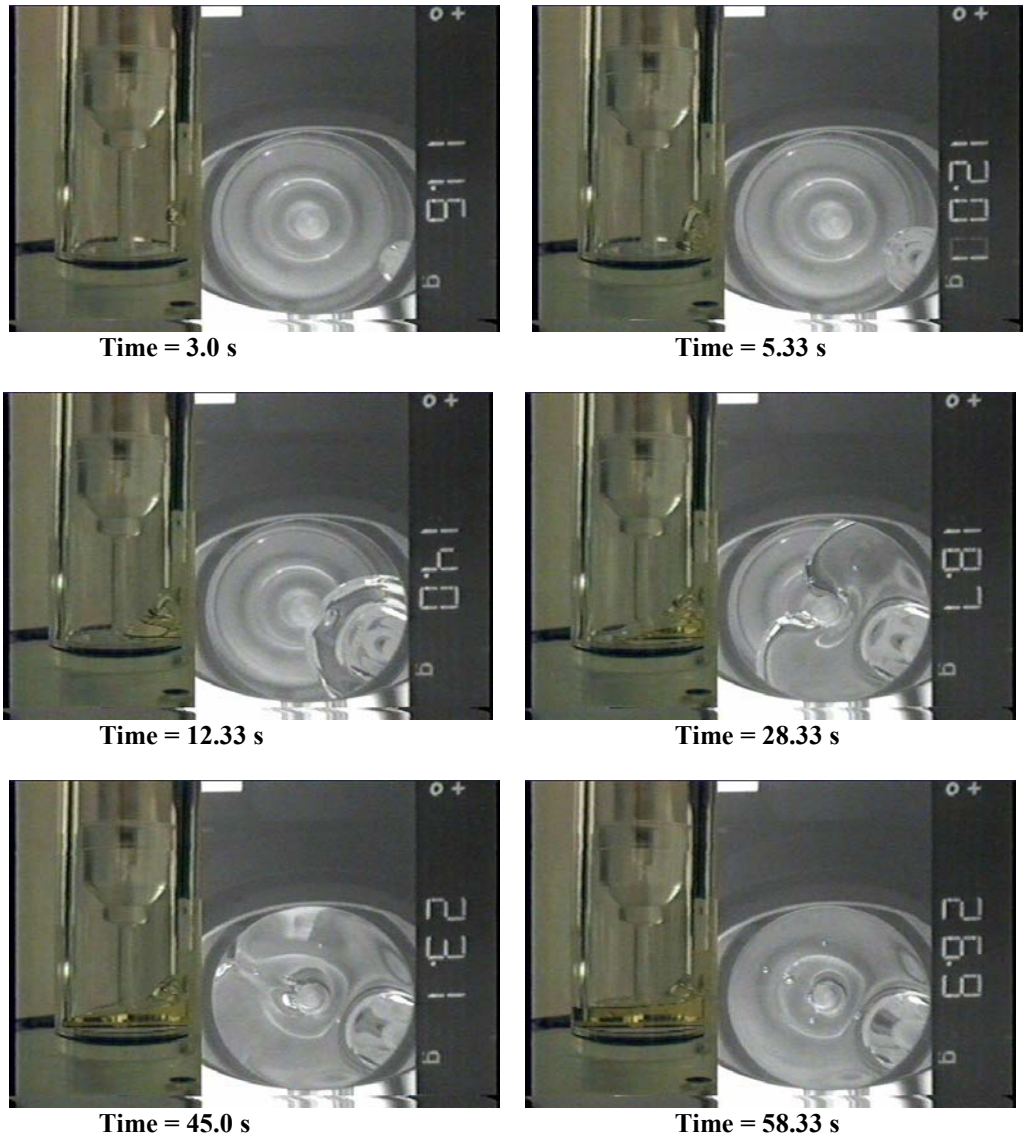

Time = 3.0 s **Time = 5.33 s**

Time = 12.33 s **Time = 28.33 s**

Time = 45.0 s **Time = 58.33 s**

Figure 5. Representative frames taken during the filling of the simple mold with UCON 75-H-90000. The far left view of each frame shows the shape of the fluid interface as it enters the mold from the right. The center view is up from the bottom. The far right view is of the scale monitoring the weight of the fluid.

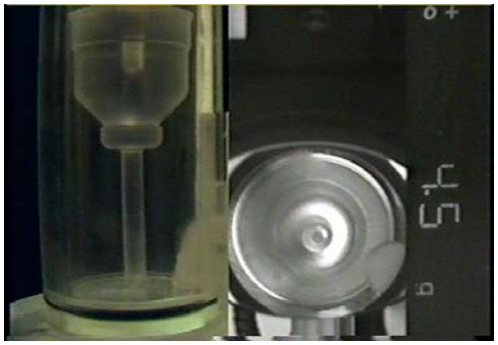

Time = 3.0 s

Time = 5.33 s

Time = 7.33 s

Time = 12.33 s

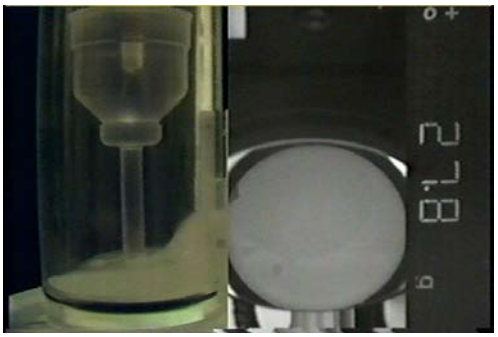

Time = 28.33 s

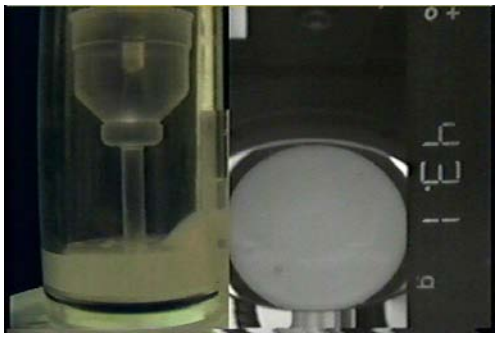

Time = 45.0 s

Figure 6**.** Representative frames taken during the filling of the simple mold a suspension of 45% by volume Alox particles in Jeffamine T5000. The far left view of each frame shows the shape of the fluid interface as it enters the mold from the right. The center view is up from the bottom. The far right view is of the scale monitoring the weight of the fluid.

.

Time = 0.5 s **Time = 1.0 s**

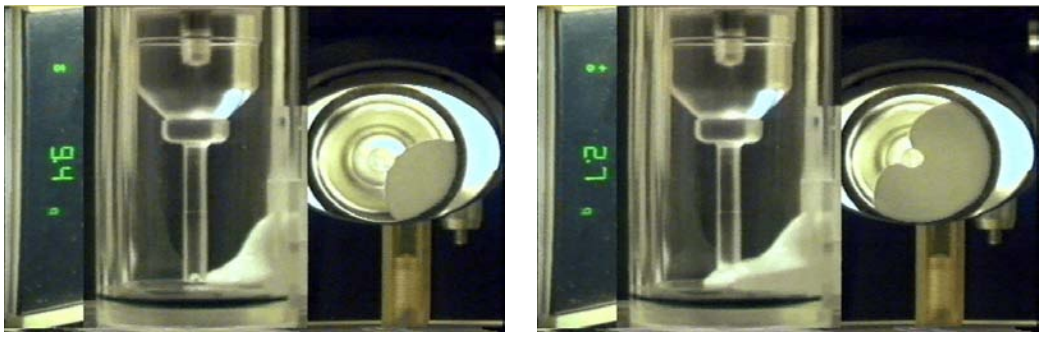

Time = 1.4 s **Time = 3.0 s**

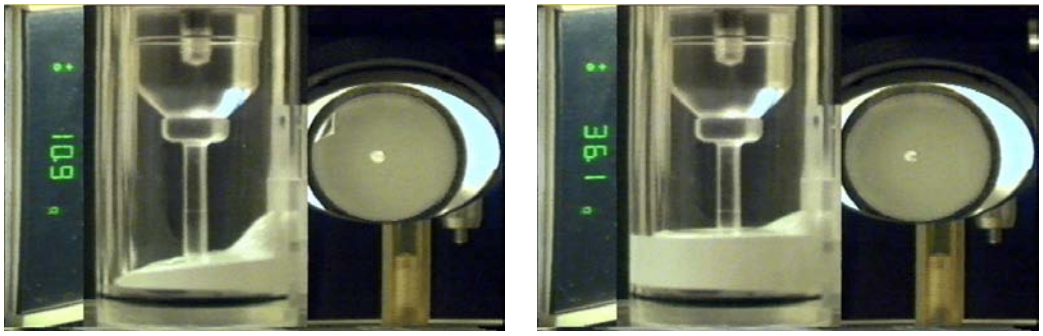

Time = 5.33 s **Time = 12.33 s**

Figure 7. Representative frames taken during the filling of the simple mold with a suspension of 45% by volume Alox particles in Jeffamine T403. The scale does not register correctly for the first 2 seconds as it is responding to the vibration of the valve opening.

3. Nuclear Magnetic Resonance Imaging

3.1 Experimental details

Nuclear Magnetic Resonance (NMR) imaging was also used for flow visualization of suspension flow into a mold with the same geometry as described above. Several changes to the process were required to go from the visual recording to using this imaging technique. The apparatus must fit in the bore (approximately 10 cm diameter) of a superconducting magnet (Figure 8) and can include no metal parts. To protect the NMR magnet and electronics from an accidental spill, the top of the mold was not left open but included a vent line near the top of the mold. Both the mold and the liquid reservoir were machined from a single block of Plexiglas™. Also the apparatus was redesigned for remote operation of the filling valve. Figure 9 shows a sketch of the apparatus.

The NMR imaging technique requires a few seconds per image in order to get a better signal-to-noise ratio. Therefore, a much slower flow rate was needed and the corresponding pressure was too low to be accurately controlled with our existing pressure regulator. Instead we used a second reservoir to create a small head of water connected to the line labeled “supply” in Figure 9.

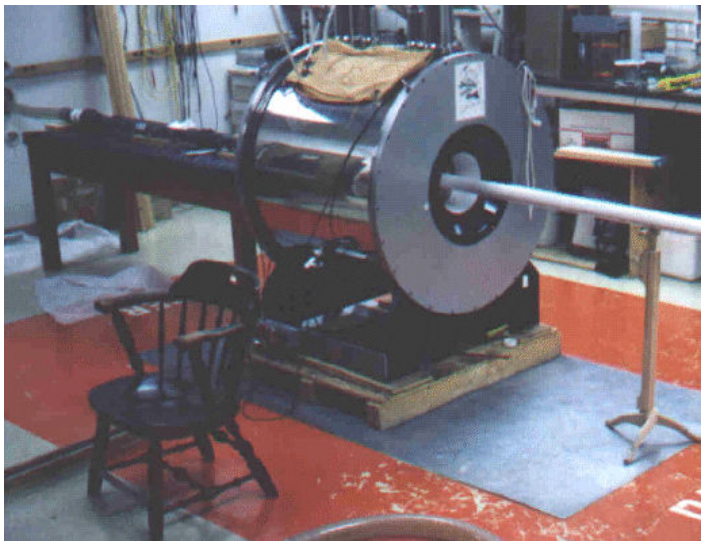

Figure 8. Photo of superconducting magnet

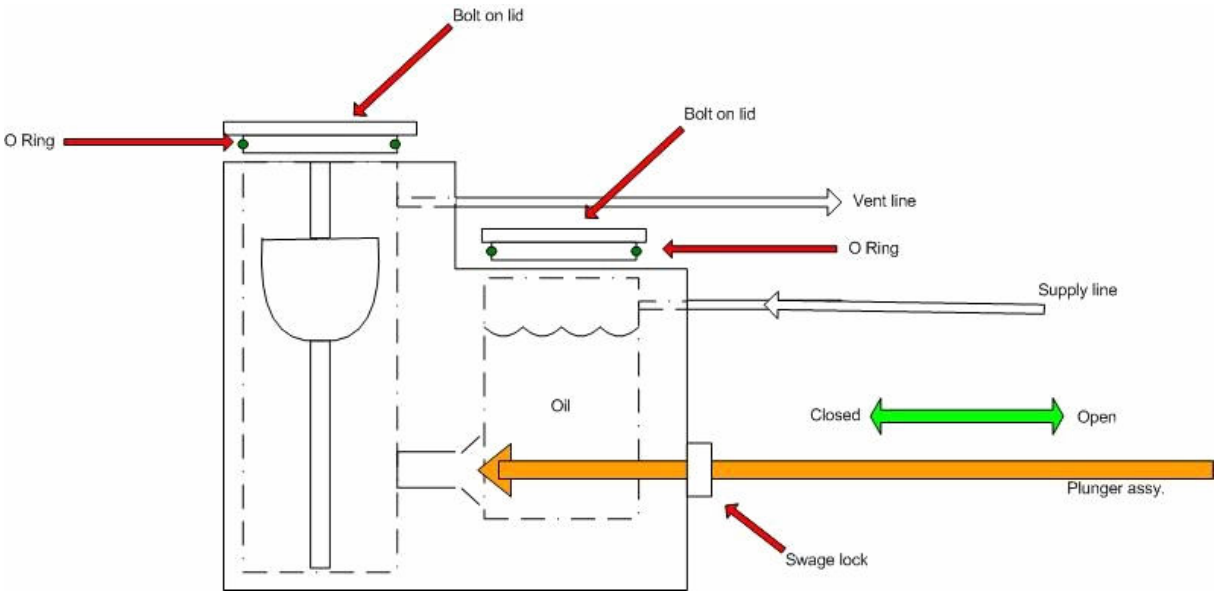

Figure 9. Sketch of mold used in NMR experiments

The strength of the NMR technique is its ability to distinguish the solid and liquid phases and, therefore, to give a direct measurement of the solids concentration. In order to devise an experiment that would be a serious test of suspension constitutive equations, we used particles larger than the Alox and, therefore, expected to exhibit flow induced migration. The system was 65% by volume of UCON 50-HB-5100 and 35% by volume of polystyrene particles. At 20°C the UCON 50-HB-5100 viscosity is 3.6 Pa-s and the density is 1.056 g/cc, which approximately matches the density of the polystyrene particles. No noticeable floating or settling occurred in the suspension over several days. The particles were sieved by the manufacturer between standard sieve sizes of 20 and 40 mesh, corresponding to a nominal diameter of 638 μm (the average of the mesh opening sizes of these two sieves).

An NMR imaging sequence was devised to image a slice parallel to the axis of the cylindrical mold and bisecting both the cylinder and fill port. The nominal volumetric flow rate was calculated from the images to be 0.25 ml/s.

3.2 Results

Figure 10 shows representative frames of the NMR movie. Each time listed is actually the time of the mid-point of the imaging sequence. The shape of the interface can be seen at early times, but because of the inherent time averaging of the technique these shapes are less accurate than those that can be obtained from the visual imaging described in the last section.

However, NMR imaging allows changes in the particle concentration to be determined. Lighter areas of the images correspond to higher liquid fraction and lower particle fraction. Note that directly above the fill port a region of lower particle concentration forms. This propagates upward as the fill progresses, leading to an asymmetric particle

concentration in the gap between the mold walls and the wine glass. Below the fill port another line of low particle concentration also forms, leaving an area of slightly higher particle concentration between this line and the bottom of the mold.

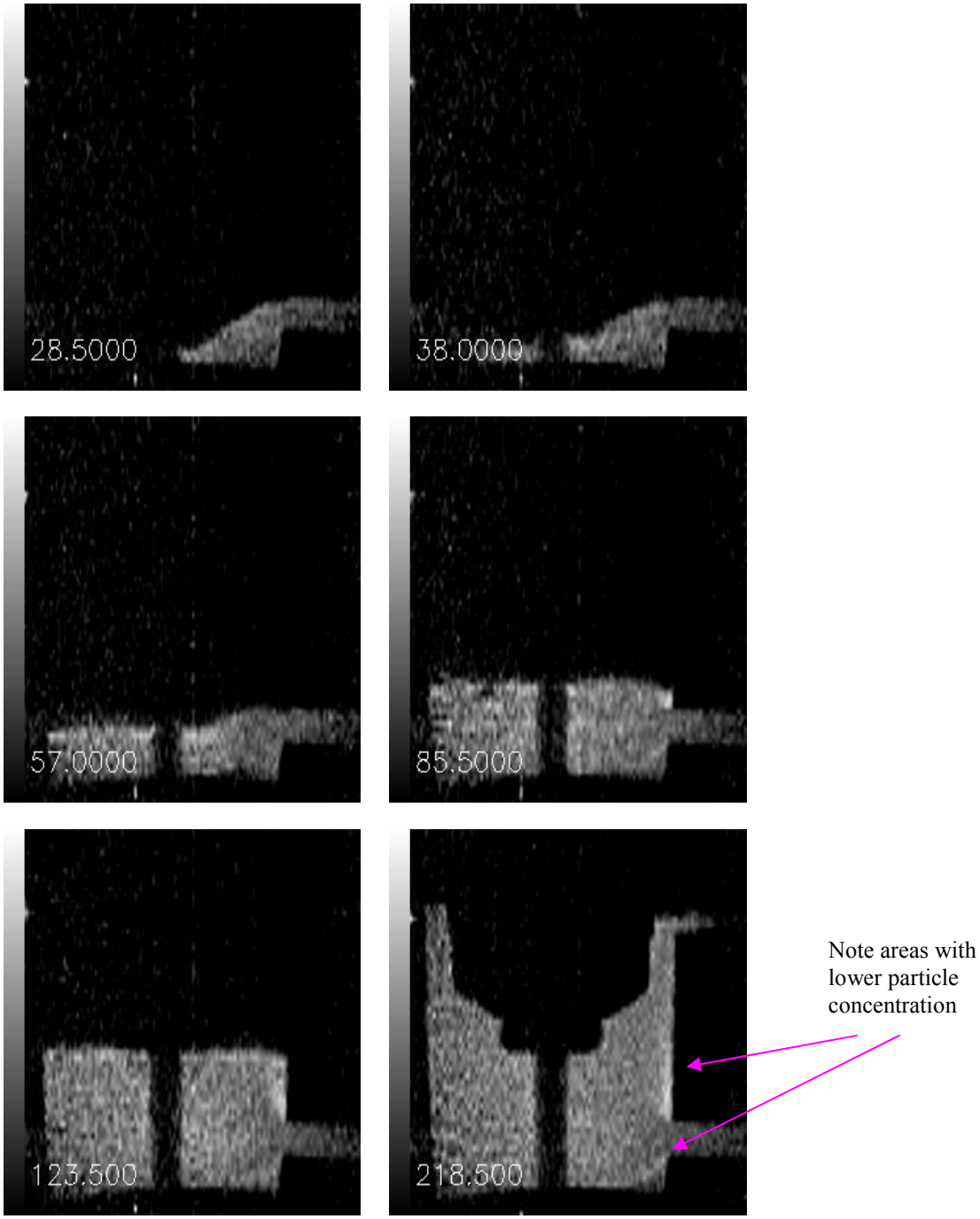

Figure 10. NMR images of a suspension of 35% by volume of polystyrene particles in UCON 50-HB-5100 lubricant filling a cylindrical mold around a wine glass insert. Numbers indicate the time in seconds. The bright areas along the wall immediately above the fill port, in a stripe diagonally down from the fill port, and along the edges the wine glass are areas of lower particle concentration.

This page intentionally left blank

4. Conclusions

A series of flow visualization experiments have been completed to provide validation data for modeling mold filling. Two mold shapes were used: one with a cylindrical outer shape and only a simple "wine glass" internal object; the other with an asymmetric, squarer outer shape and several internal shapes. This report gives the results of experiments filling the former mold.

Three classes of fluids were used: single phase lubricants; suspensions of large, ideal particles in Newtonian lubricants; or a model of the 459 encapsulant consisting of tabular alumina particles in a viscous Jeffamine. The classes of fluids were chosen to allow validation of the computational models of the free surface flow assuming either simple Newtonian or suspension constitutive equations. Ideal suspensions of relatively large particles neutrally buoyant in a Newtonian viscous fluid were used to provide a rigorous test of models using the diffusive flux particle migration constitutive equation (Fang et al. 2002, Rao et al. 2002). Suspensions of alumina powder were also used to provide tests for more complex rheological models that capture shear history effects (Rao et al. 2003, Grillet et. al. 2005). Rheological and wetting properties of these fluids were collected for use as input parameters for the computational models.

The videos show the shape of the interface as the fluid enters the mold. The videos also can provide metrics such as the time it takes for the fluid to reach a certain object or for the interface to meet when the flow is split around an obstacle. Furthermore, NMR images provide information about particle migration in a mold-filling flow.

Part 2 describes the continuation of this study, using a more realistic geometry. Here a significant finding was that air bubbles introduced into the flow consistently accumulated under the wine glass shape.

This page intentionally left blank

5. References

Adolf, Doug, Mark Stavig, and Howard Arris, "Viscosity Test Results from 459 with ALOX, GMB, and Mica Fillers," memo to Barb Wells (Feb. 28, 2000).

Baer, Thomas A., David R. Noble, Rekha R. Rao, and Anne M. Grillet, "A Level Set Approach to 3D Mold Filling of Newtonian Fluids," Proceedings of the ASME Symposium on Flows in Manufacturing Processes, Honolulu, Hawaii, July 6-10, 2003.

Fang, Z., M. S. Ingber, A. Mammoli, J. F. Brady, M. S. Ingber, L. A. Mondy, and A. L. Graham, "Flow-Aligned Tensor Models for Suspension Flows," *Int. J. Multiphase Flow* **28**, 137 (2002).

Grillet, Anne M., Rekha R. Rao, Stacie Kawaguchi, Douglas B. Adolf and Lisa A. Mondy, "Complex Rheology and Modeling of Composite Materials," Journal of Rheology, paper in preparation 2005.

Rao, R. R., L. A. Mondy, P. R. Schunk, P. A. Sackinger, D. B. Adolf, "Verification and Validation of Encapsulation Flow Models in GOMA, Version 1.1," Sandia National Laboratories report SAND2001-2947, October 2001.

Rao, R. R., L. A. Mondy, A. Sun, and S. Altobelli, "A Numerical and Experimental Study of Batch Sedimentation and Viscous Resuspension," *Int. J. Numerical Methods in Fluids* **39**, 465 (2002).

Rao, Rekha R., Douglas B. Adolf and Lisa A. Mondy, "Complex Rheology In Particle-Laden Composite Materials," Proceedings of the ASME Symposium on Flows in Manufacturing Processes, Honolulu, Hawaii, July 6-10, 2003.

Wilkes, E. D. and Rekha R. Rao, "On the 3D simulation of the liquid encapsulant during oven curing of a non-axisymmetric neutron generator," Memo to Distribution, in preparation 2005.

Distribution:

1	MS0384	Art Ratzel	9100
1	MS0515	Todd Haverlock	2561
1	MS0515	Barb Wells	2561
1	MS0521	Steve Montgomery	2564
1	MS0825	Wahid Hermina	9110
1	MS0834	Justine Johannes	9112
1	MS0834	Jaime N. Castañeda	9112
1	MS0834	Ray Cote	9112
1	MS0834	Anne Grillet	9112
1	MS0834	Joel Lash	9114
5	MS0834	Lisa Mondy	9114
1	MS0834	Rekha Rao	9114
1	MS0869	Dolores Sanchez	14422
1	MS1310	Steve Kempka	9113
1	MS9018	Central Technical Files	8945-1
2	MS0899	Technical Library	9616